

Reduced frequency and size of late-twenty-first-century snowstorms over North America

Walker S. Ashley ¹ Alex M. Haberlie ² and Vittorio A. Gensini ¹

Understanding how snowstorms may change in the future is critical for estimating impacts on water resources and the Earth and socioeconomic systems that depend on them. Here we use snowstorms as a marker to assess the mesoscale fingerprint of climate change, providing a description of potential changes in winter weather event occurrence, character and variability in central and eastern North America under a high anthropogenic emissions pathway. Snowstorms are segmented and tracked using high-resolution, snow water equivalent output from dynamically downscaled simulations which, unlike global climate models, can resolve important mesoscale features such as banded snow. Significant decreases are found in the frequency and size of snowstorms in a pseudo-global warming simulation, including those events that produce the most extreme snowfall accumulations. Early and late boreal winter months show particularly robust proportional decreases in snowstorms and snow water equivalent accumulations.

nowstorms and other winter weather events can affect all sectors of the economy, as well as produce considerable sensible weather effects on flora and fauna¹⁻³. It is important to consider how these snow events may shift in an Earth-atmosphere system with ongoing and anticipated change, especially since these events contribute to and sustain the cryosphere. Climatological work on past snow events has been hampered by data inconsistencies, artifacts and classification issues^{4,5}. Results from these efforts suggest that there were more extreme and more widespread snowstorms in recent decades in the United States^{1,2} with overall negative trends in maximum seasonal snow depth, snowcover extent and snow water equivalent (SWE) over North America since the 1960s6. Much of the research assessing the future response of snowfall to climate change has used coarse global climate model (GCM) output to assess changes in SWE, snow-versus-rain ratios and daily, monthly and seasonal snowfall means and extremes under warming regimes. This research suggests that, as GHG concentrations and surface temperatures increase, a smaller proportion of precipitation will fall as snow^{7,8}, mid-latitude locations will generally experience less snowfall⁷⁻¹⁰, and there will be a delay of the mean onset of the snow season¹¹ and an overall shorter snow season^{7,12}. While daily snowfall events and seasonal snowfall are projected to decrease across the Northern Hemisphere mid-latitudes under warming regimes, there is some inconsistency on whether snowfall events will become more intense¹¹⁻¹³. Although there is considerable research on many aspects of changes in the cryosphere, there has been limited work¹²⁻¹⁴ on objectively identifying, tracking and assessing how individual snow events may change in a future climate due to the incongruence of timescales between snowstorms and the coarse horizontal grid spacing of the typical GCM output used. Assessing how these events—which can cover the spectrum from minor snow accumulations, to an average winter storm, to a crippling blizzard—may change in the future has not been assessed at the snowstorm scale across a continental domain.

We investigate the contemporary central and eastern North America snowstorm climatology and how that climatology may

change during the twenty-first century using a unique event-tracking algorithm on existing high-resolution (hourly, 4-km horizontal grid spacing), dynamically downscaled regional climate model output¹⁵. High-resolution, convection-permitting, dynamically downscaled simulations overcome many of the shortcomings of GCMs (for example, poor representation of topography leading to underestimation of snow16 and errors and uncertainties affiliated with convective parametrization¹⁷), allowing more accurate representation of mesoscale processes and features critical to weather extremes such as banded snow and lake-effect snow 12,18. A current drawback of these simulations is their substantial computational expense and the resulting time necessary to produce, store and process output. These limitations hinder the production of extensive periods to analyse, with most dynamically downscaled simulation research limited to about a decade of output available for comparison. This limited evaluation period for a single scenario reduces our capability of exploring the full spectrum of the possible changes to the climate system. Another caveat of the simulations is the pseudo-global warming (PGW) approach used, which does not permit examination of potential changes to the general circulation from a GCM. Instead, in the PGW approach, lateral boundary conditions and sea surface temperatures are perturbed by a climate change signal. By not incorporating GCM projected changes due to, for example, arctic warming and melting sea ice19, the PGW approach does not permit the assessment of decadal and interdecadal oceanic and atmospheric phenomena that may influence the climate system^{20–22}.

The key variable in the simulation output that is tracked is SWE, which is the water-equivalent snow depth accumulation, in millimetres, for the previous hour. This variable provides a representation of where it is snowing and the snow's water-equivalent magnitude. SWE 'swaths', which are the footprints of snowstorms, are tracked (Extended Data Fig. 2) for historical periods (2000–2013) and prospective future periods (forced under representative concentration pathway RCP 8.5). The initial epoch is used as an early-twenty-first-century control (CTRL) and a perturbed,

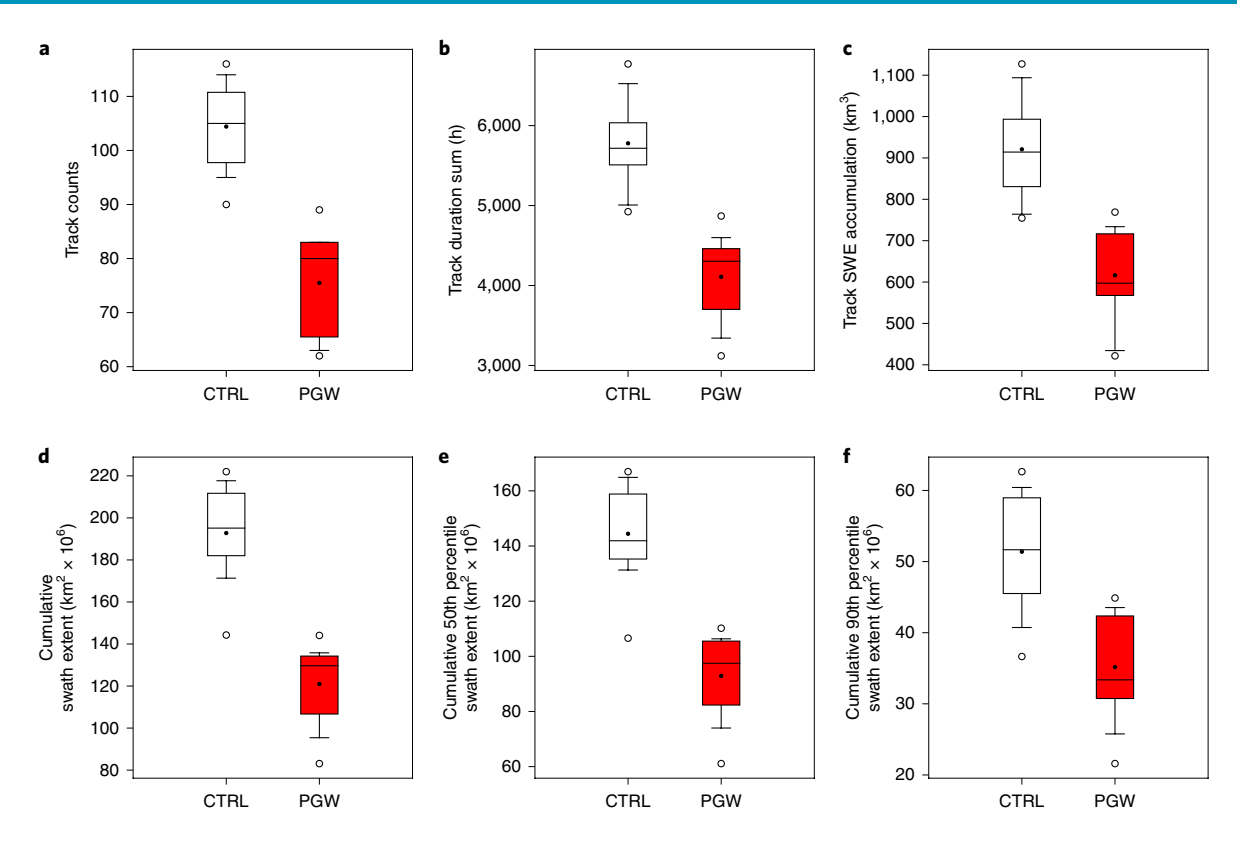


Fig. 1 | Seasonal comparisons between CTRL and PGW. a-f, Seasonal comparisons between CTRL and PGW. Seasonal variability over the study period for select track statistics: total counts (a), sum of durations (b), SWE accumulation (c), maximum extent (d), maximum 50th percentile extent (e) and maximum 90th percentile extent (f). Means are denoted by black dots and medians are denoted by the black lines. The boxes illustrate the interquartile range, the whiskers represent the 5th and 95th percentiles, and the clear circles denote outliers.

PGW approach was used to simulate weather for a potential late-twenty-first-century, high-emission climate pathway. SWE data were missing for February 2005 in the simulation output; therefore, we removed the 2004-2005 season from analysis, resulting in a total of 12 winter seasons assessed in each simulation. Although the performance of seasonal snowfall/snowcover/snowpack, extreme precipitation and other precipitation characteristics of the CTRL was vetted previously¹⁵, we compared the SWE climatology of the CTRL to an observed SWE climatology and found that the simulation outputs were representative of observations, especially for areas of highest mean SWE values (Extended Data Fig. 1). We are most interested in assessing how snowfall events of various accumulation thresholds differ between the historical period and PGW-perturbed simulations. Ultimately, the measured change, or delta, in snowstorm attributes between the experiments provides a unique view of how climate change may affect future cryosphere inputs. Any changes in these events could alter albedo feedbacks of snowcover, surface energy budgets, water cycle efficiency, water resources, and physical, biological and social environments²³.

Here we show that seasonal results reveal major differences between the CTRL and PGW snowstorm track counts and total swath-based SWE over central and eastern North America (Fig. 1 and Supplementary Information). In all cases, there were significant decreases in both seasonal snowstorm counts (k=1.0, P<0.001) and SWE totals (k=0.92, P<0.001) from the CTRL to PGW simulation. Over the 12-yr period, there were ~30 fewer snowstorms or a decline of nearly 28%, per year in PGW compared to CTRL. The maximum and minimum snowstorm counts for CTRL were 116 and 90, respectively, while the maximum and minimum storm counts for PGW were 89 and 62, respectively. This suggests that in future warming scenarios (for example, PGW), even seasons that produce

the largest count of snow events still may not exceed the lowest frequency years in the early twenty-first century. These results are similar for SWE. CTRL SWE totals per year range from 754.7 to 1,126.7 km³, whereas PGW SWE totals per year range from 421.6 to 769 km³. On average, future cool seasons produce ~300 km³, or 33%, less frozen precipitation in these events across the study domain. An examination of snowstorm attributes reveals some insight into the statistical drivers of these changes. The maximum extent of snowstorms showed a significant areal reduction of over 37% between CTRL and PGW (k=0.092, P<0.001). On average, storms tracked in the PGW scenario have a total swath area that is ~240,000 km² smaller—equivalent to the surface area of the Great Lakes—than those storms in the CTRL. Seasonal cumulative snowstorm swath hours have significantly different distributions in the PGW run compared to CTRL (k=1, P < 0.001), resulting in a mean decline of 29%. Interestingly, the distributions of durations (k = 0.05, P = 0.22) and SWE (k = 0.04, P = 0.23) for future and present snowstorms are not significantly different. Overall, these results suggest that the significant reduction in seasonal SWE is caused by fewer future snowstorms and events that generally have smaller areal footprints.

Spatially, the CTRL and PGW simulations generate an expected latitudinal gradient in snow event frequency (Fig. 2a,b), with the highest event totals across the upper Great Lakes, southeast Canadian Shield and Hudson Bay Lowlands. The northern High Plains of the United States to the Great Lakes and into New England experienced ~16–32 snow events a year during the early twenty-first century but the PGW simulations suggest that this frequency may decrease by 6–15 events (30–50%) annually by the end of the century under a high-end climate pathway (Fig. 2c,d). Previous research¹³ found similar proportional declines in daily snowfall events projected by GCMs forced by RCP 8.5 for the late

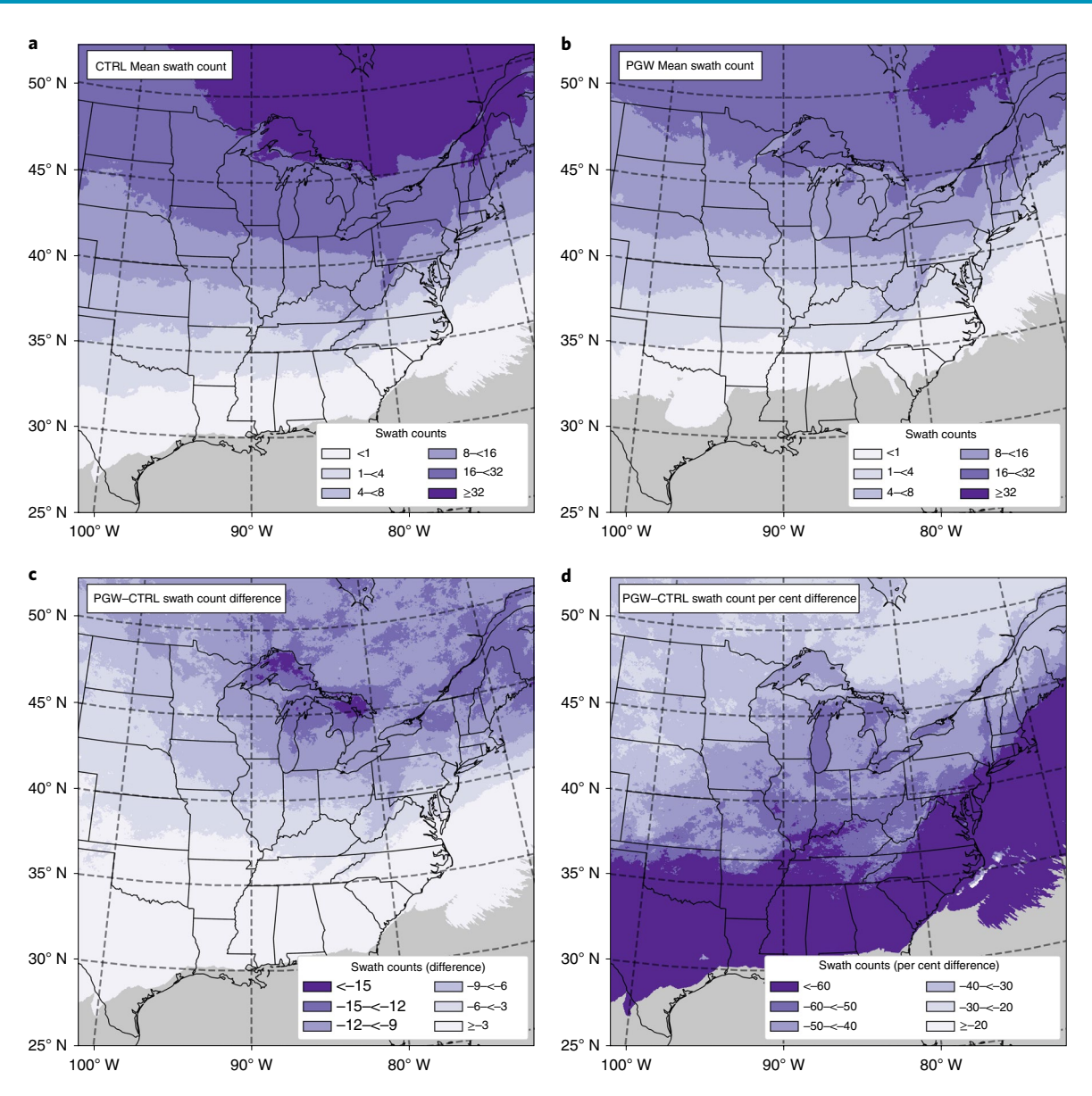


Fig. 2 | Spatial climatology of snow events. a-d, Mean annual swath counts (a,b) and swath count difference (c) and per cent difference (d) between CTRL (a) and PGW (b). The areas in grey experienced no qualifying swaths during the study period.

twenty-first century. Seasonal SWE from Minnesota eastward to the Canadian Maritimes is projected to decrease from 50 to $100\,\mathrm{mm}$ (Extended Data Fig. 3) which, using a simple 10:1 snow-to-liquid ratio, is nearly a decline of $50-100\,\mathrm{cm}$ in snow accumulation. Areas of the St Lawrence Valley, Maine and New Brunswick are expected to see a decline of $>100\,\mathrm{mm}$ in SWE under RCP 8.5.

The greatest reduction in snow events is found in the northern Great Lakes (Fig. 2c), probably due to the PGW simulation lessening lake ice cover and effective accumulation substrate, which, in turn, reduces the snow event footprint across the lakes. Lake-effect and lake-enhanced precipitation are often affiliated with larger cyclones and may be captured as part of some events that traversed the region in the simulation output, although the algorithm removes isolated lake-effect cases since they do not meet spatial thresholds for a 'snowstorm'. Despite the projected decline in event frequency of the Great Lakes, SWE downwind of Lake Superior increases in the PGW simulation, which may be due to expected dramatic declines in lake ice and greater dynamically induced wind fetch increasing evaporation and leading to greater lake-enhanced precipitation

in the late century¹⁸. An upward trend in snowfall and SWE has already been identified downwind of Lake Superior in the twentieth century⁴ and the CTRL and PGW simulation comparisons suggest that this will continue (Extended Data Fig. 3). Conversely, a decline in snow event and affiliated SWE in the snowbelts of Lake Erie and Ontario is expected in the late twenty-first century as more precipitation falls as rain due to projected regional warming²⁴.

Proportionally, the largest decline in snow events is projected along and south of the Ohio River and Ozark Plateau (Fig. 2d), regions that historically experience relatively few snow events each year. Despite the relative minimum in snowstorms in the southern United States, when events do occur, the impacts can be substantial to the built environment². Winter weather events and affiliated impacts in this humid subtropical region are projected to become extremely rare, with notable declines in snow events in the region's elevated terrain (for example, along the Cumberland Plateau and in the southern Appalachians), which, historically, experienced relatively high event totals (Fig. 2c). These climatologically warmer regions have a strong marine influence, which fosters temperatures

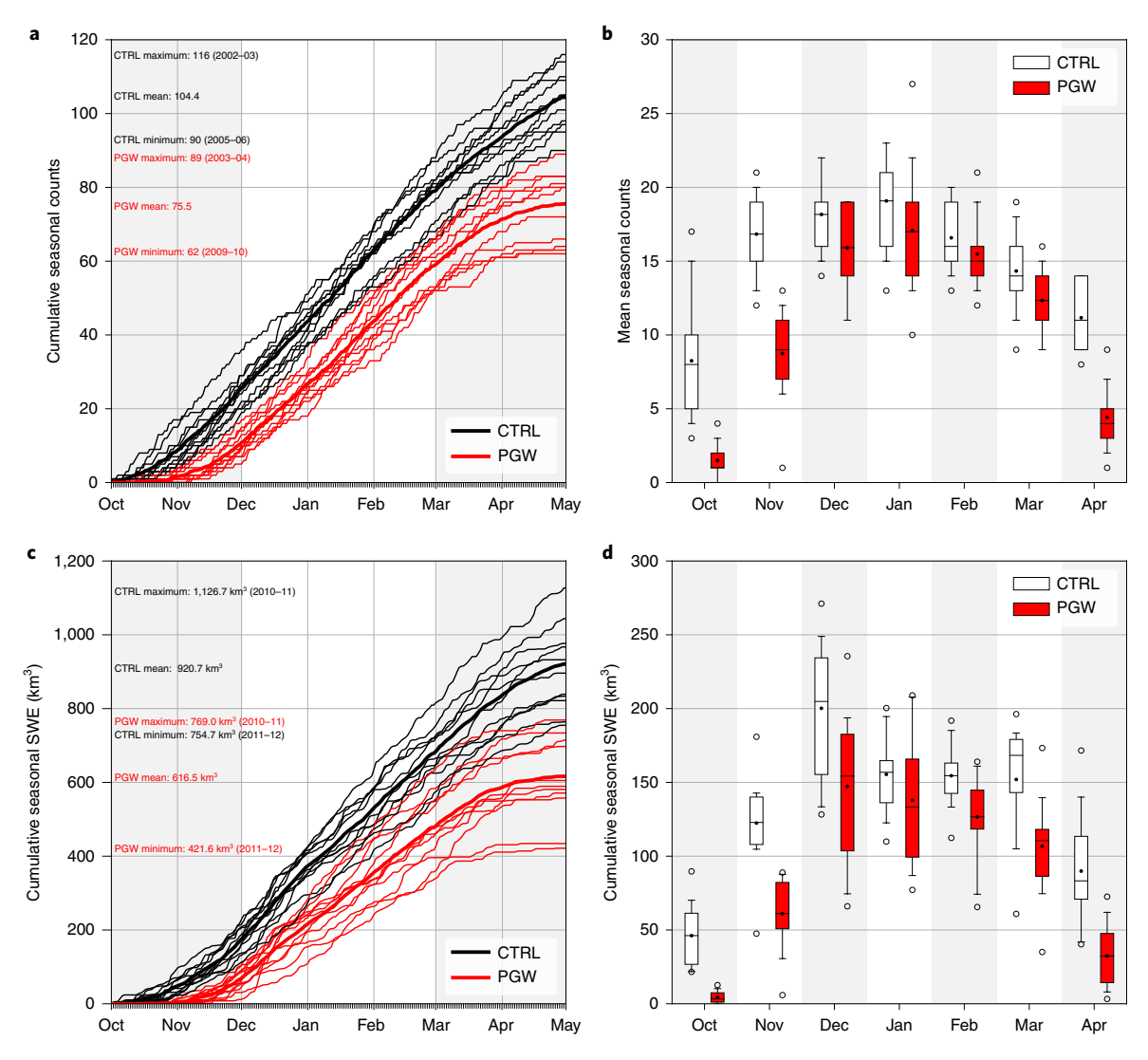


Fig. 3 | Snow event counts. a-d, Seasonal (a,c) and subseasonal (b,d) variability in swath counts (a,b) and snow water equivalents (SWE) (c,d) per season (October-April) for CTRL (black lines and white boxes) and PGW (red lines and red boxes). Means are denoted by thicker lines (a,c) and black dots (b,d). For b and d, medians are denoted by the black lines, the boxes illustrate the interquartile range, the whiskers represent the 5th and 95th percentiles and the clear circles denote outliers. Cumulative swath counts (a) and SWE totals (c) are recalculated daily for each season and the maximum, mean and minimum values are reported on the left side of each panel.

that are already marginal for snowfall in the present climate $^{7,12}.$ As the climate warms, precipitation is projected to increasingly fall as rain since snow-supportive environments will diminish at these latitudes $^{10,12}.$ Although proportional changes in the poleward latitudes are smaller, these are areas that have historically long-lived snow-cover 23 and high seasonal SWE where any notable drop in snowfall inputs could have important implications. Most of these northward locations have declines in SWE of 20–40% from the CTRL to the PWG scenarios, which corresponds to SWE magnitude losses of 25–100 mm or 25–100 cm of snow accumulation using a 10:1 snow-to-liquid ratio.

The most notable changes between the CTRL and PGW simulations arise during the shoulder-season months (Fig. 3); temperatures during these months are marginal for snowfall and the fraction of precipitation falling as snow is especially sensitive to warming due to climate change^{7,12}. Snowstorm counts during October, November and April are projected to decrease 83.5%, 48.4% and 60.5%, respectively, signalling a robust decrease in future events during the shoulder seasons and a further shortening of the already observed changes

in spring snowcover across the Northern Hemisphere²⁵. The largest per cent reduction in all metrics is found during October, suggesting that future early season snow events will be nearly eliminated if RCP 8.5 is realized. Monthly swath count decreases of 5.1-12.8% are projected during the core of winter, revealing declines in snowstorms even during the coldest months. These reductions in winter month counts are affiliated with even larger proportional losses in snowstorm swath hours and SWE totals. These changes are underscored by examining the weekly per cent differences in swath counts, total SWE and SWE area (Fig. 4). The per cent reduction in weekly storm counts maximizes in October, with most PGW weeks experiencing 0-20% of the counts produced by the CTRL. This PGW count deficit stabilizes between 80% and just over 100% of CTRL storms during meteorological winter. Although meteorological spring shows smaller deficits compared to autumn, most PGW weeks in March and April only generate 50% of the mean weekly snowstorm counts produced in CTRL. Similar patterns exist for SWE, underlining the direct effect these reduced counts may have on regional hydroclimates during the autumn and spring.

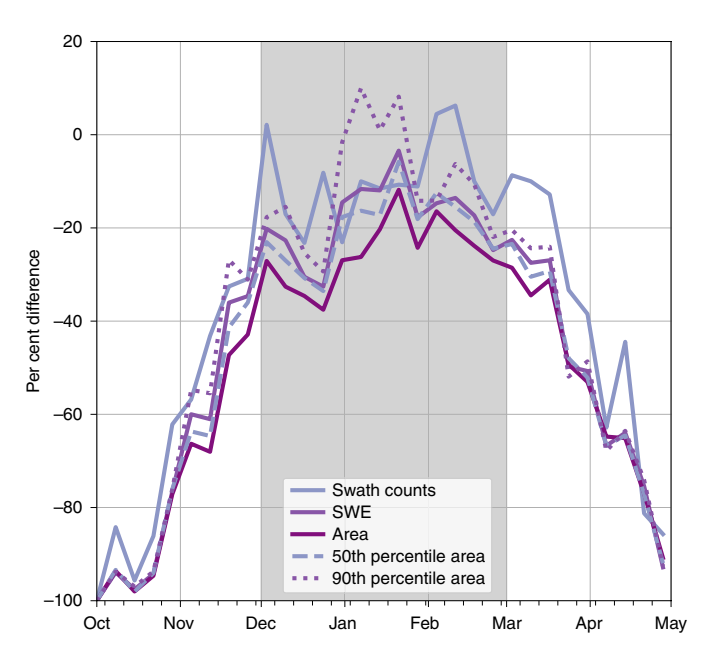


Fig. 4 | Weekly per cent difference between the two epochs. Per cent difference between CTRL and PGW (100 × (PGW/CTRL - 1)) for the weekly sums of swath counts, SWE and snowstorm areal extent for all 3-h SWE rates, as well as 50th and 90th percentile rates.

To evaluate changes in the more intense areas of snowstorms, we assessed each detected snow swath for SWE pixels that exceeded the 50th percentile (moderate intensity) and 90th percentile (extreme intensity) for 3-h SWE accumulations. There was a 35.9% and 32.0% decline in the 50th and 90th percentile areal extent of snowstorms, respectively, from the CTRL to the PGW scenarios. Paralleling the results found in the overall event swaths, the most dramatic declines in moderate (intense) areas from the CTRL to PGW scenarios were found in the shoulder seasons, with >90% (90%) decrease in these areas in October, around a 58% (52%) decline in November and 69% (70%) drop in April. All months registered decreases in moderate and intense snowstorm areas, except for a negligible or 0.3%, increase in the 90th percentile for January. Overall, there was a statistically significant mean reduction in 50th percentile (k=0.07, P=0.012) and 90th percentile (k=0.08, P=0.001) snowstorm footprint area, with an average reduction of 152,000 km² (26,000 km²) per storm, or roughly the area of Michigan (Maryland), no longer showing these intense snowfall rates in the PGW scenario. Spatially, 90th percentile events are projected to decrease across the study domain on a seasonal basis, with the greatest proportional reductions found equatorward of 40°N stretching into the Coastal Northeast (Extended Data Fig. 4). However, for the midwinter months of January and February, these extreme intensity events are projected to increase in the northern Great Plains of the United States and southern Canadian Prairies (Extended Data Fig. 5); this matches the future midwinter pattern found recently in GCM output12. Due to increases in global annual surface evaporation, these higher latitudes will experience more abundant moisture in the future²⁶, which may result in more frequent intense snowstorms in the midwinter when temperatures in these poleward locations will remain supportive of snow, even in a warmer climate¹².

Much of the past work on the potential climatological changes of Northern Hemisphere snow has focused on seasonal or longer-term assessments of the cryosphere^{8,25,27-30}. While there have been some assessments in potential changes to extratropical cyclone frequency, paths and intensity^{20–22,31,32}, only a few recent efforts^{12–14,33} have used relatively coarse spatiotemporal data to begin to understand

how snow accumulations on shorter timescales may change in the future. Using a snow event-tracking method on high-resolution downscaled simulation output, this study presented an approach to understanding how snowstorms may change in the twenty-first century. Applying automated image segmentation procedures, we were able to extract the spatiotemporal characteristics of 2,159 snow events across central and eastern North America in two simulation epochs. This method afforded a unique description of possible changes in winter weather event occurrence and variability in the twenty-first century under a high-end GHG pathway. Results from the event-based analysis are consistent with recent work that has assessed relatively coarse snowfall output from GCMs^{7,8,10,12-14}.

Study findings revealed the potential for substantial change in the frequency and character of North American snowstorms; such changes will have far-reaching implications on energy budgets, the hydrologic cycle and all sectors of the economy, especially if high-end emission scenarios are realized³⁴⁻³⁶. Snowstorm counts, swath hours and SWE magnitudes had significant declines from the CTRL to PGW simulations. The most notable declines in snowstorm counts were found during the shoulder seasons, where projections reveal a near complete removal of events in a future high-end warming pathway. Even the most intense parts of snowstorms as measured by high accumulation rates have reductions of >30% in the PGW scenario. Contractions in future snowstorm counts, spatiotemporal traits and SWE magnitudes could have positive outcomes by reducing built environment impacts and acute human system impacts, notably on air and road transportation systems. Conversely, a reduction in future cryospheric inputs could have adverse consequences, especially for freshwater resource-dependent industries such as agriculture, power generation, river and lake transport, refining, manufacturing and recreation^{34,36}. Any changes in the magnitude and timing of snowstorms and the snowfall/rainfall ratio³⁷, will directly influence snowpack, snowmelt and energy budgets, as well as the timing, frequency and degree of hazards such as flood and drought^{38,39}.

Study limitations include a relatively short period of analysis due to the computational expense of dynamical downscaling and the use of a PGW approach, which does not permit an evaluation of possible changes in the general circulation. Although computationally expensive, future research should simulate additional years and anthropogenic emission pathways to provide a more comprehensive picture of future snowstorm prospects across North America. Additionally, future simulations could explore the use of GCM inputs instead of perturbed reanalyses. This would allow further examination into the dynamic influence of climatic change on large-scale circulation patterns^{19–22} and the subsequent downscaled impact on snowstorm production. Finally, to fully explain why snowstorms may change in the future, additional research should assess the shifts in snowstorm-supportive environments between the two epochs. Identifying how these environments are changing is critical for understanding why the North American snowstorm landscape will change in the twenty-first century.

Online content

Any methods, additional references, Nature Research reporting summaries, source data, extended data, supplementary information, acknowledgements, peer review information; details of author contributions and competing interests; and statements of data and code availability are available at https://doi.org/10.1038/s41558-020-0774-4.

Received: 16 September 2019; Accepted: 8 April 2020; Published online: 25 May 2020

References

 Changnon, S. A. & Changnon, D. A spatial and temporal analysis of damaging snowstorms in the United States. Nat. Hazards 37, 373–389 (2006).

- Squires, M. F. et al. The regional snowfall index. Bull. Am. Meteorol. Soc. 95, 1835–1848 (2014).
- 3. Coleman, J. S. M. & Schwartz, R. M. An updated blizzard climatology of the contiguous United States (1959–2014): an examination of spatiotemporal trends. *J. Appl. Meteor. Climatol.* **56**, 173–187 (2017).
- Kunkel, K. E. et al. Trends in 20th century U.S. snowfall using a quality-controlled data set. J. Atmos. Oceanic Technol. 26, 33–44 (2009).
- Kunkel, K. E. et al. Monitoring and understanding trends in extreme storms: state of knowledge. Bull. Am. Meteorol. Soc. 94, 499–514 (2013).
- Kunkel, K. E. et al. Trends and extremes in Northern Hemisphere snow characteristics. Curr. Clim. Change Rep. 2, 65–73 (2016).
- Krasting, J. P., Broccoli, A. J., Dixon, K. W. & Lanzante, J. R. Future changes in Northern Hemisphere snowfall. J. Clim. 26, 7813–7828 (2013).
- O'Gorman, P. A. Contrasting responses of mean and extreme snowfall to climate change. *Nature* 512, 416–418 (2014).
- Diffenbaugh, N. S., Scherer, M. & Ashfaq, M. Response of snow-dependent hydrologic extremes to continued global warming. *Nat. Clim. Change* 3, 379–384 (2012).
- Kapnick, S. B. & Delworth, T. L. Controls of global snow under a changed climate. J. Clim. 26, 5537–5562 (2013).
- Notaro, M., Lorenz, D., Hoving, C. & Schummer, M. Twenty-first-century projections of snowfall and winter severity across Central-Eastern North America. J. Clim. 27, 6526–6550 (2014).
- Danco, J. F., DeAngelis, A. M., Raney, B. K. & Broccoli, A. J. Effects of a warming climate on daily snowfall events in the Northern Hemisphere. J. Clim. 29, 6295–6318 (2016).
- Janoski, T. P., Broccoli, A. J., Kapnick, S. B. & Johnson, N. C. Effects of climate change on wind-driven heavy-snowfall events over eastern North America. J. Clim. 31, 9037–9054 (2018).
- Zarzycki, C. M. Projecting changes in societally impactful northeastern U.S. snowstorms. Geophys. Res. Lett. 45, 12067–12075 (2018).
- 15. Liu, C. et al. Continental-scale convection-permitting modeling of the current and future climate of North America. *Clim. Dynam.* **49**, 71–95 (2017).
- Rasmussen, R. et al. High-resolution coupled climate runoff simulations of seasonal snowfall over Colorado: a process study of current and warmer climate. J. Clim. 24, 3015–3048 (2011).
- Prein, A. F. et al. Simulating North American mesoscale convective systems with a convection-permitting climate model. *Clim. Dynam.* 1432-0894, 1–16 (2017).
- 18. Notaro, M., Bennington, V. & Vavrus, S. Dynamically downscaled projections of lake-effect snow in the Great Lakes basin. *J. Clim.* **28**, 1661–1684 (2015).
- Cohen, J., Pfeiffer, K. & Francis, J. A. Warm arctic episodes linked with increased frequency of extreme winter weather in the United States. *Nat. Commun.* 9, 869 (2018).
- Chang, E. K. M. CMIP5 projection of significant reduction in extratropical cyclone activity over North America. J. Clim. 26, 9903–9922 (2013).
- Eichler, T. P., Gaggini, N. & Pan, Z. Impacts of global warming on Northern Hemisphere winter storm tracks in the CMIP5 model suite. *J. Geophys. Res.* Atmos. 118, 3919–3932 (2013).

- Tamarin-Brodsky, T. & Kaspi, Y. Enhanced poleward propagation of storms under climate change. Nat. Geosci. 10, 908–913 (2017).
- Vaughan, D.G. et al. in Climate Change 2013: The Physical Science Basis (eds Stocker, T. F. et al.) Ch. 4 (IPCC, Cambridge Univ. Press, 2013).
- Suriano, Z. J. & Leathers, D. J. Twenty-first century snowfall projections within the eastern Great Lakes region: detecting the presence of a lake-induced snowfall signal in GCMs. Int. J. Climatol. 36, 2200–2209 (2016).
- Brown, R. D. & Robinson, D. A. Northern Hemisphere spring snow cover variability and change over 1922–2010 including an assessment of uncertainty. *Cryosphere* 5, 219–229 (2011).
- Collins, M. et al. in Climate Change 2013: The Physical Science Basis (eds Stocker, T. F. et al.) Ch. 12 (IPCC, Cambridge Univ. Press, 2013).
- Déry, S. J. & Brown, R. D. Recent Northern Hemisphere snow cover extent trends and implications for the snow-albedo feedback. *Geophys. Res. Lett.* 34, L22504 (2007).
- Choi, G., Robinson, D. A. & Kang, S. Changing Northern Hemisphere snow seasons. J. Clim. 23, 5305–5310 (2010).
- Brown, R. D. & Mote, P. W. The response of Northern Hemisphere snow cover to a changing climate. J. Clim. 22, 2124–2145 (2009).
- Brutel-Vuilmet, C., Ménégoz, M. & Krinner, G. An analysis of present and future seasonal Northern Hemisphere land snow cover simulated by CMIP5 coupled climate models. Cryosphere Discuss. 6, 3317–3348 (2012).
- Colle, B. A. et al. Historical evaluation and future prediction of eastern North American and western Atlantic extratropical cyclones in the CMIP5 models during the cool season. J. Clim. 26, 6882–6903 (2013).
- Ma, C.-G. & Chang, E. K. M. Impacts of storm-track variations on wintertime extreme weather events over the continental United States. *J. Clim.* 30, 4601–4624 (2017).
- Zhou, B., Wang, Z., Shi, Y., Xu, Y. & Han, Z. Historical and future changes of snowfall events in China under a warming background. *J. Clim.* 31, 5873–5889 (2018).
- 34. IPCC Climate Change 2014: Impacts, Adaptation, and Vulnerability (eds Field, C. B. et al.) (Cambridge Univ. Press, 2014).
- Mankin, J. S. et al. The potential for snow to supply human water demand in the present and future. *Environ. Res. Lett.* 10, 114016 (2015).
- Impacts, Risks, and Adaptation in the United States: Fourth National Climate Assessment Vol. II (eds Reidmiller, D. R. et al.) 24–32 (USGCRP, 2018).
- Trenberth, K. E. Changes in precipitation with climate change. Clim. Res. 47, 123–138 (2011).
- Climate Change 2013: The Physical Science Basis (eds Stocker, T. F. et al.) (IPCC, Cambridge Univ. Press, 2013).
- Climate Science Special Report: Fourth National Climate Assessment Vol. I (eds Wuebbles, D. J. et al.) (USGCRP, 2017).

Publisher's note Springer Nature remains neutral with regard to jurisdictional claims in published maps and institutional affiliations.

 $\ensuremath{\texttt{©}}$ The Author(s), under exclusive licence to Springer Nature Limited 2020

Methods

Dynamical downscaling output. We use simulation output. generated by Liu et al. and described by Prein et al. to reveal recent and potential future changes in the central and eastern North American snow event climatology. High-resolution, convective permitting simulations such as those produced by Liu et al. are desired for climate change studies that wish to assess changes in extreme mesoscale phenomena. Simply, extremes—such as, in our case, intense snow bands and lake-effect/enhanced snows—are affiliated with and/or driven by mesoscale processes, which are not resolved well in GCMs. For instance, snowfall is underestimated in GCMs due to poor grid representation of topography, land cover and water. Additionally, GCMs require convective parameterization, which are often too simple to accurately represent complex processes that are not well understood and are sources of errors and uncertainties. High-resolution, convection-permitting simulations overcome many of the shortcomings of GCMs, permitting more accurate representation of mesoscale processes and features critical to local weather extremes.

The Liu et al.¹⁵ simulations used a dynamical downscaling technique that used original and modified ERA-interim⁴⁷ data as initial and lateral boundary conditions to force the Advanced Research Weather Research and Forecasting (WRF-ARW) model v.3.4.1 (ref. ⁴⁸). After initial testing by Liu et al. ¹⁵, refined model physics were implemented to mitigate snowpack underprediction, excessive production of lake-effect precipitation and a cool-season temperature bias found near the Great Lakes. The unmodified ERA-interim data was used as an early-twenty-first-century CTRL, with output stretching from October 2000 to September 2013. Next, a perturbed, PGW approach was used to simulate weather for a potential late-twenty-first-century, high-emission climate pathway or RCP 8.5 (refs. 49,50). In this scenario, initial and boundary conditions were derived from reanalysis and adjusted by adding the CMIP5 ensemble mean of the RCP 8.5 (see supplementary table 1 in Liu et al.¹⁵). Resulting outputs are relatively high spatiotemporal resolution (hourly output, 4-km horizontal grid spacing) and, as illustrated in previous work^{15,41}, reproduce accurately the location, evolution and intensity of precipitating systems during the historical period. Specifically relevant to work here, Liu et al.15 found that, compared to observations, the historical simulation captures particularly well the spatial patterns and magnitudes of cool-season precipitation, especially in the central and eastern United States (see figs. 5 and 6 in Liu et al.15).

Snow events are tracked using the SWE output from the simulations. This output is generated every hour and provides reasonable representation of where it is snowing and the intensity of the snow in the simulation. SWE is used as a snowfall proxy since snow accumulation outputs were not saved from the Liu et al. 15 simulations.

Snow water equivalent verification. To assess any potential SWE bias in the simulation, we compared CTRL SWE output for the October-April 2003-2013 period to NOAA National Operational Hydrologic Remote Sensing Center's SNOw Data Assimilation System (SNODAS^{51,52}) output. The 2004–2005 season was omitted from this comparison due to missing WRF data. The SNODAS assimilates in situ and remotely sensed data to generate the best-possible estimates of snowcover and associated parameters⁵³. Daily 6:00 UT snapshots of SNODAS SWE were used to serve as ground truth for comparison with the temporally overlapping CTRL SWE output. After creating mean period SWE climatology (Extended Data Fig. 1b), absolute difference values were calculated and expressed as a percentage difference of the SNODAS total mean SWE (Extended Data Fig. 1b). This analysis indicates that areal mean SWE totals are representative, especially in the areas of highest mean SWE values. Differences >30% between the simulations are noted roughly south of the 35° N parallel, where mean SWE totals are an order of magnitude smaller than most of the northern CONUS totals. Compared to SNODAS, the actual mean amounts showed a systematic low SWE bias across most of the northern Plains, Midwest and Northeast of the United States. The largest mean differences between CTRL and SNODAS were found in New York and throughout New England. This is not a perfect comparison due to the documented limitations and biases of SNODAS54 but it does provide evidence that the CTRL simulation adequately captures the climatological distribution of SWE observations. In addition, the main goal herein is to evaluate the potential delta between the historical period and PGW-perturbed simulations, not to produce bias correction estimates.

Snow event tracking. Initially, our algorithm segments 3-hourly 'slices' of snow events (Extended Data Fig. 2b). Slices are identified by selecting simulation grid points that meet or exceed 0.1 mm SWE for a 3-h period, which, using a simple 10:1 snow-to-liquid ratio, is \sim 1 mm of snow accumulation. To be considered a snow event slice, grid points meeting the 0.1 mm 3-hourly SWE intensity threshold must be connected and each connected region must exceed an area of \sim 100 km². Slices are then concatenated to produce snow event swaths. These swaths represent the snow footprint of a winter weather event and can be used to determine the snow accumulation produced by a 'snowstorm'. Swaths are generated by testing for spatiotemporal overlap between slices identified in SWE fields from successive 3-h periods. Ties (for example, multiple slices overlap between time steps) are broken by selecting the slice with the most similar attributes (for example, area

and major axis length) to the last valid slice in an ongoing swath. Once the swaths are generated, the first and last time steps in which their slices had an area of at least $1\times10^5\,\mathrm{km^2}$ (roughly the size of the state of Kentucky) are identified. If the amount of time between these time steps is at least 24 h, the swath is included in this study. These values are chosen on the basis of the minimum temporal and spatial thresholds that represent the synoptic scales. Within each swath, pixels that exceed the 50th (Fig. 1c) and 90th (Fig. 1d) percentiles for 3-h SWE accumulations are identified for the purposes of determining the spatiotemporal occurrence these events. The percentiles are calculated on the basis of the values for all pixels meeting or exceeding the 0.1-mm 3-h SWE threshold in the CTRL dataset for October–April in areas east of the Continental Divide. The 3-h values for the 50th and 90th percentiles are 0.46 mm (~4.6 mm snow) and 2.08 mm (~20.8 mm snow), respectively. All products presented in this study (except for Extended Data Fig. 2) are derived from SWE data from the period between the first and last instances of slices with areas of at least $1\times10^5\,\mathrm{km^2}$ within qualifying swaths.

The algorithm is used to track thousands of winter weather events produced by the simulations across a domain roughly east of the 1,500-m elevation found on the leeside of the Rocky Mountains, bounded on the east by ~60° W, on the north by 55°N and on the south by 20°N. By using this domain, we remove the complexities affiliated with tracking snow events in the variable terrain found west of the Continental Divide and, instead, reveal the character of snow events produced by leeside and coastal cyclones of central and eastern North America. By comparing snow event attributes generated from the early-twenty-first-century output (CTRL) with the late-twenty-first-century output (PGW), a climatological difference in events between the study periods was produced. Within this domain, the tracked CTRL (PGW) snowstorms accounted for 80% (75%) of the October-April SWE accumulations for the 12-yr period. This suggests that the tracked entities are very important aspects of the cool-season hydroclimate within the study area. Spatially, this contribution maximizes over the Great Plains and Southeastern Canada and minimizes over the Great Lakes. This is expected due to the small size and somewhat transient nature of lake-effect snow events.

Statistical analysis. All statistical tests use the non-parametric, two-sample, Kolmogorov–Smirnov test with an alpha of 0.05 for comparing numerical distributions. We report the so-called Kolmogorov–Smirnov statistic (k) and the P value. We report an exact P if it is >0.001. If this is not the case, we report P as <0.001. The reported result that there were significant decreases in both seasonal snowstorm counts and SWE totals is based on the seasonal counts of snowstorms and the SWE produced by those storms (n=12) and these values can be found in Supplementary Table 1. For all statistical tests involving per-snowstorm statistics, n was 1,253 for CTRL and 906 for PGW (total snowstorm counts).

SWE volume is reported in km³. This value is calculated by finding the per-grid sum of SWE (mm) in each 3-h snapshot within qualifying snowstorms. This value is then converted to km by multiplying the sum by 10^{-6} . This can be thought of as the total depth of all SWE if it were concentrated on one grid. Next, this value is multiplied by the area of one grid, which is approximately the product of the grid spacing in two dimensions $(4 \times 4 \, \text{km}^2)$. These values range from 0.24 to $75.72 \, \text{km}^3$. Snowstorm area, or the maximum areal extent of the snowstorm, is calculated by counting all grid cells that experience at least one 3-h period in which a qualifying snowstorm produced at least 0.1 mm of SWE. The reported area is computed by multiplying the count of all grids that meet this criterion for each storm by the specified grid spacing $(4 \times 4 \, \text{km}^2)$. These values range from 169,456 to $7,209,664 \, \text{km}^2$. The grid spacing is based on the reported lambert conic conformal distance. As with all areal calculations within an expansive study area, these areas are approximations.

Data availability

The dynamically downscaled simulation output is available from NCAR's Research Data Archive⁴⁰.

Code availability

The source code 56 for the snow event identification and tracking is available from https://github.com/ahaberlie/Future_Snow.

References

- High Resolution WRF Simulations of the Current and Future Climate of North America (NCAR, accessed 1 April 2018); https://rda.ucar.edu/datasets/ ds612.0/
- 41. Prein, A. F. et al. Increased rainfall volume from future convective storms in the U.S. *Nat. Clim. Change* 7, 880 (2017).
- Déqué, M. et al. An intercomparison of regional climate simulations for Europe: assessing uncertainties in model projections. *Clim. Change* 81, 53–70 (2007).
- Michaelis, A. C., Willison, J., Lackmann, G. M. & Robinson, W. A. Changes in winter North Atlantic extratropical cyclones in high-resolution regional pseudo-global warming simulations. *J. Clim.* 30, 6905–6925 (2017).
- 44. Musselman, K. N. et al. Projected increases and shifts in rain-on-snow flood risk over western North America. *Nat. Clim. Change* 8, 808–812 (2018).

- Michaelis, A. C. & Lackmann, G. M. Climatological changes in the extratropical transition of tropical cyclones in high-resolution global simulations. J. Clim. 32, 8733–8753 (2019).
- Scaff, L. et al. Simulating the convective precipitation diurnal cycle in North America's current and future climate. Clim. Dynam. https://doi.org/10.1007/ s00382-019-04754-9 (2019).
- 47. Dee, D. P. et al. The era-interim reanalysis: configuration and performance of the data assimilation system. O. J. R. Meteorol. Soc. 137, 553–597 (2011).
- Powers, J. G. et al. The weather research and forecasting model: overview, system efforts, and future directions. *Bull. Am. Meteorol. Soc.* 98, 1717–1737 (2017).
- Rasmussen, K., Prein, A., Rasmussen, R., Ikeda, K. & Liu, C. Changes in the convective population and thermodynamic environments in convection-permitting regional climate simulations over the United States. *Clim. Dynam.* 0930–7575, 1–26 (2017).
- Meinshausen, M. et al. The RCP greenhouse gas concentrations and their extensions from 1765 to 2300. Clim. Change 109, 213–241 (2011).
- Carroll, T. et al. NOHRSC Operations and the Simulation of Snow Cover Properties for the Conterminous U.S. (NOAA, 2001); http://snobear.colorado. edu/WSC/WSC_2001/PDF/WSC2001CarrollEtAl.PDF
- Barrett, A. National Operational Hydrologic Remote Sensing Center Snow Data Assimilation System (SNODAS) Products at NSIDC (NSIDC, 2003); https:// nsidc.org/sites/nsidc.org/files/files/nsidc_special_report_11.pdf
- Snow Data Assimilation System (SNODAS) Data Products at NSIDC Version 1 (NSIDC, accessed 5 December 2019); https://doi.org/10.7265/N5TB14TC
- Clow, D. W., Nanus, L., Verdin, K. L. & Schmidt, J. Evaluation of SNODAS snow depth and snow water equivalent estimates for the Colorado Rocky Mountains, USA. *Hydrol. Process.* 26, 2583–2591 (2012).
- Markowski, P. & Richardson, Y. Mesoscale Meteorology in Midlatitudes Ch. 1 (John Wiley & Sons, 2010).

 Haberlie, A. M. ahaberlie/Future_Snow: 2020.2 (Zenodo, 2020); https://doi. org/10.5281/zenodo.3674139

Acknowledgements

We thank K. Ikeda and A. Prein for their assistance in accessing and interpreting the Liu et al. 15 output. This research was supported by National Science Foundation grant no. ATM-1637225.

Author contributions

W.A. conceived the study. A.H. and W.A. led on the design of the study and analysed the data. A.H. constructed the tracking algorithm. V.G. led on the simulation output verification. All authors contributed to writing the manuscript, with W.A. as lead manuscript author and A.H. as lead author for the Methods.

Competing interests

The authors declare no competing interests.

Additional information

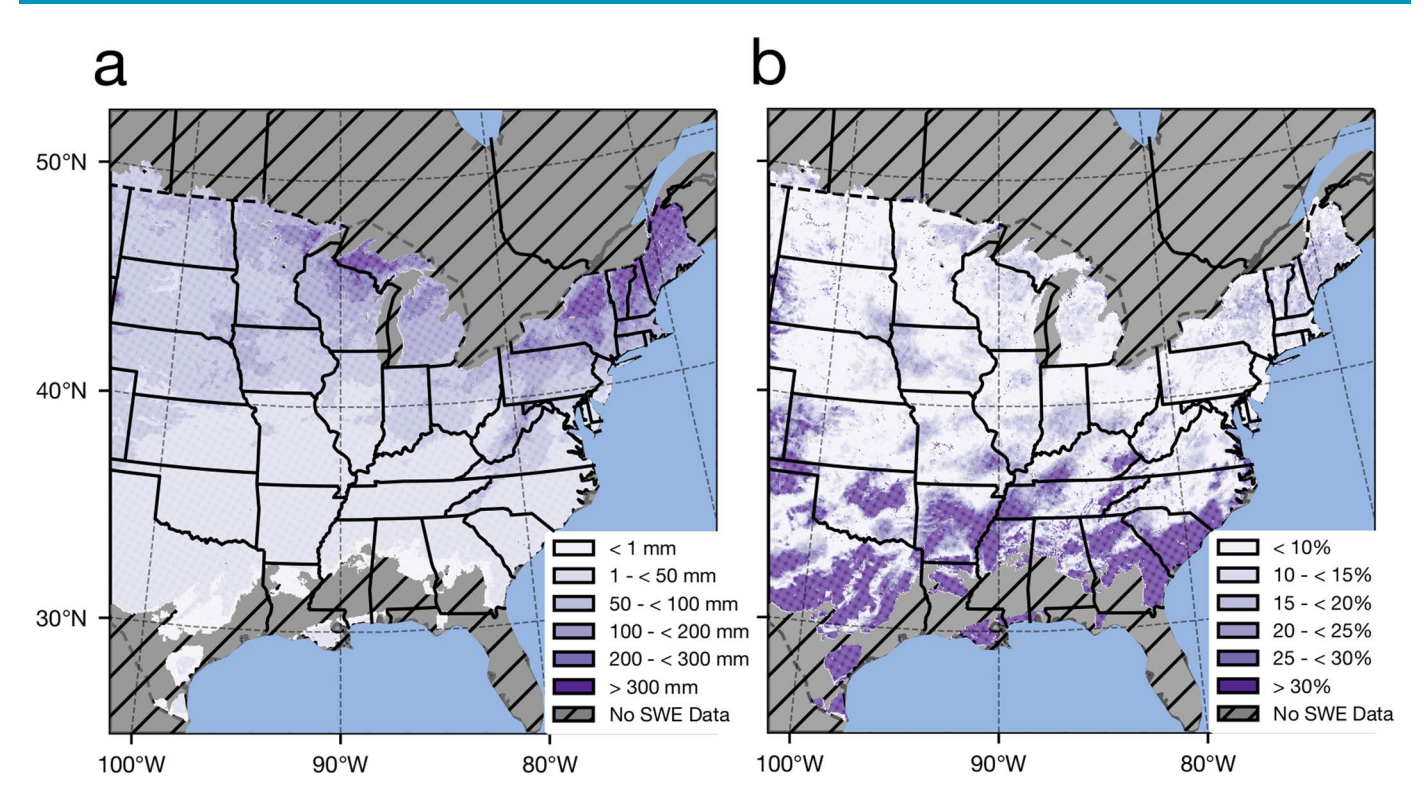
Extended data is available for this paper at https://doi.org/10.1038/s41558-020-0774-4.

Supplementary information is available for this paper at https://doi.org/10.1038/s41558-020-0774-4.

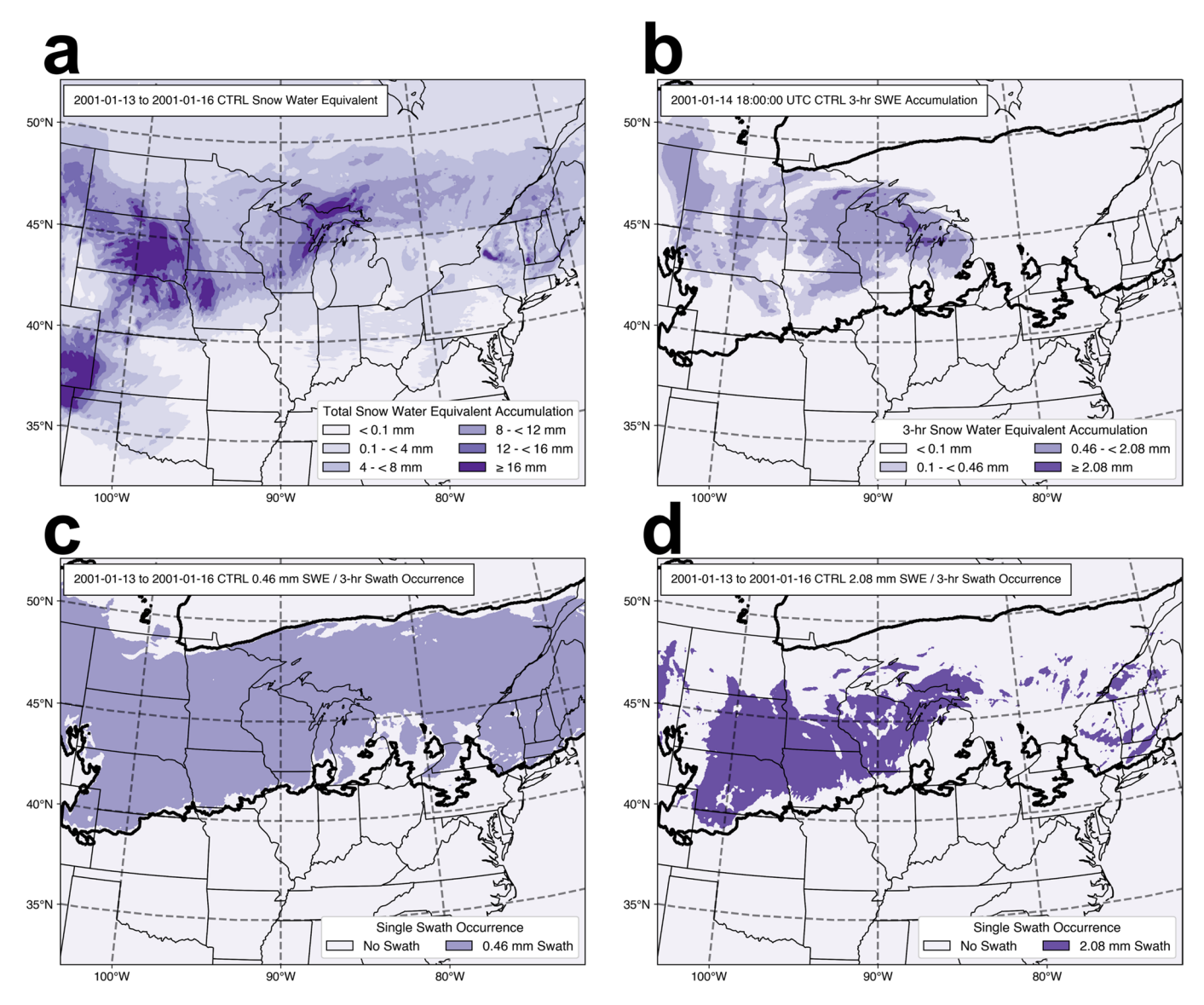
Correspondence and requests for materials should be addressed to W.S.A.

Peer review information Nature Climate Change thanks Martin Baxter, Anthony Broccoli and the other, anonymous, reviewer(s) for their contribution to the peer review of this work

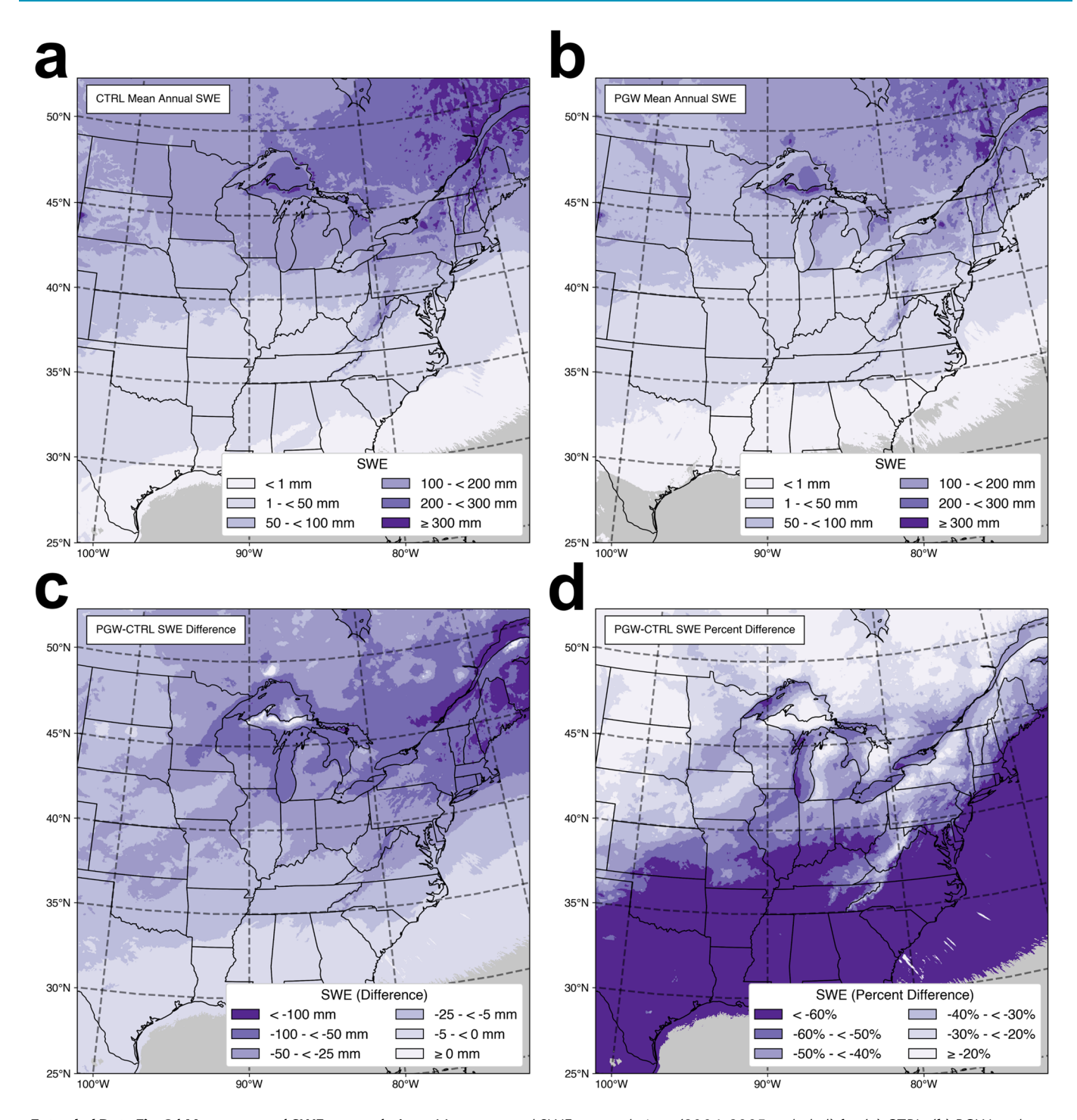
Reprints and permissions information is available at www.nature.com/reprints.



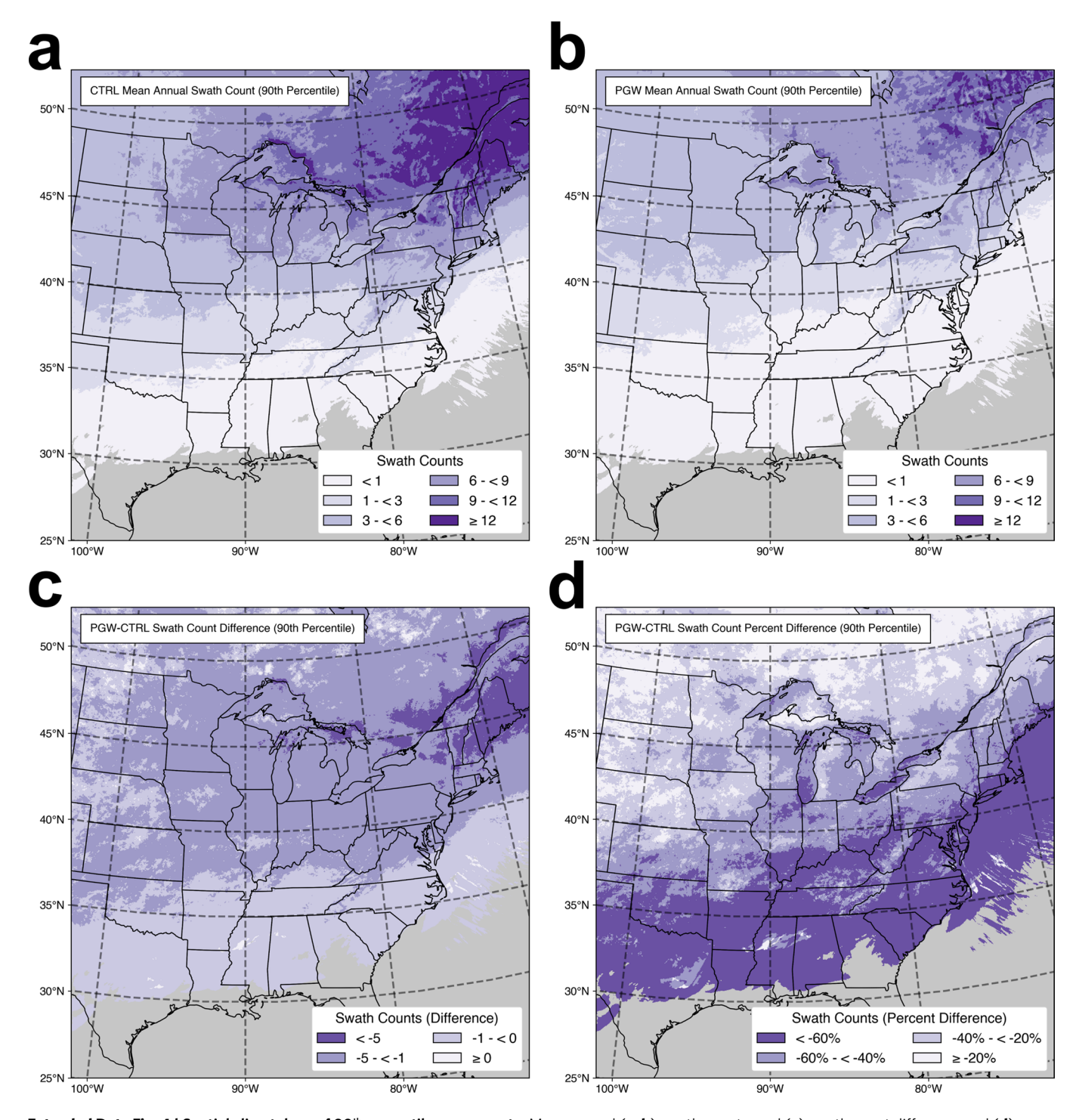
Extended Data Fig. 1 | Comparison to climatology. October-April 2003–2013 **a)** SNODAS average SWE (mm) and **b)** the absolute difference between WRF-CTRL and SNODAS mean SWE shown as a per cent of the total mean SNODAS SWE. As discussed in the manuscript, 2004–05 season was omitted from analysis due to missing WRF data. Hatched areas on both figures indicate locations where SNODAS data were not available or both WRF-CTRL and SNODAS did not record any SWE during the analysis period.



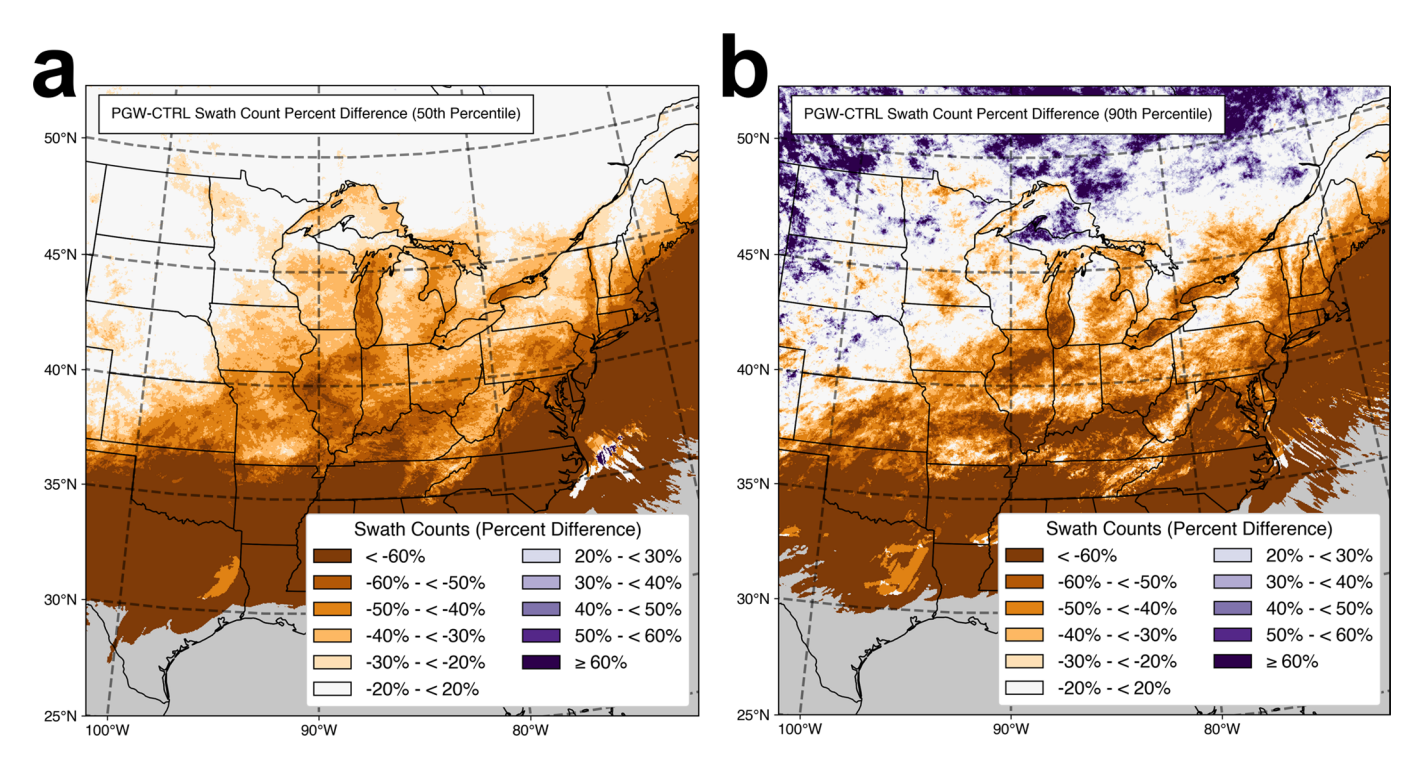
Extended Data Fig. 2 | Event detection and tracking. Demonstration of the various sources of climatological calculations from CTRL, namely, **a**) total accumulation of snow (liquid water equivalent) from January 13th 2001 to January 16th 2001, **b**) a 'slice' within a qualifying swath with the lowest (0.1mm / 3-hr), 50th percentile (0.46mm / 3-hr), and 90th percentile (2.08mm / 3-hr) snowfall totals (liquid water equivalent) denoted by the colour fill. The black outline is the spatial extent of the swath (that is, where the swath produced at least 0.1mm / 3-hr liquid water equivalent totals), **c**) the spatial extent of the occurrence of 3-hr liquid water equivalent snowfall totals exceeding the 50th percentile within this swath, and **d**) the spatial extent of the occurrence of 3-hr liquid water equivalent snowfall totals exceeding the 90th percentile within this swath.



Extended Data Fig. 3 | Mean seasonal SWE accumulations. Mean seasonal SWE accumulations (2004–2005 excluded) for (a) CTRL, (b) PGW, and accumulated SWE (c) differences and (d) per cent differences.



Extended Data Fig. 4 | Spatial climatology of 90th percentile snow events. Mean annual (**a, b**) swath counts, and (**c**) swath count difference and (**d**) percent difference between (**a**) CTRL and (**b**) PGW for only 90th percentile snow events. The areas in grey experienced no qualifying swaths during the study period.



Extended Data Fig. 5 | Per cent change in midwinter moderate and extreme intensity snowstorms. Per cent difference in (a) 50th and (b) 90th percentile swath event counts between CTRL and PGW for the months of January and February.